JOURNAL OF MATERIALS SCIENCE 24 (1989) 4437–4442

Surface reactivity of reduced $LaFeO_3$ as studied by TPD and IR spectroscopies of CO, CO_2 and H_2

V. CORTÉS CORBERÁN*, LUIS G. TEJUCA†, ALEXIS T. BELL‡
*Instituto de Catálisis y Petroleoquímica, C.S.I.C., Serrano 119, 28006 Madrid, Spain
‡Department of Chemical Engineering, University of California, Berkeley, California 94720-9989, USA
†Deceased, formerly of Instituto de Catálisis y Petroleoquímica, C.S.I.C., Serrano 119, 28006 Madrid, Spain.

CO, CO_2 and H_2 reactive adsorption on $LaFeO_3$ at 298 K has been studied as a function of the reduction temperature of the perovskite oxide by means of temperature programmed desorption (TPD) and infrared (IR) spectroscopies. TPD spectra of CO after CO adsorption contained peaks at 365 to 440 K assigned to linearly adsorbed CO and at 495 to 540 K assigned to bridged CO. TPD spectra of CO_2 after CO adsorption presented broad peaks centred at 570 and 715 K assigned to monodentate and bidentate carbonates, respectively. TPD spectra of CO_2 obtained after CO_2 adsorption contained peaks at 375 to 425 K and at 570 to 675 K. These were associated to infrared bands of monodentate and bidentate carbonates, respectively. In the CO–H_2 and H_2–CO successive adsorption on the reduced surface of $LaFeO_3$ the TPD peak of H_2 at 345 to 360 K is strongly inhibited and a new desorption peak appeared at 585 to 590 K. This is assumed to be due to CO adsorption on metallic Fe^0 sites (CO–H_2 coadsorption) or to a displacement of adsorbed hydrogen from Fe^0 to a new adsorption site (H_2–CO coadsorption). CO was found to interact more strongly than hydrogen with the adsorbent surface.

1. Introduction

Perovskite oxides have been recently used for CO and CO_2 hydrogenation [1–6]. Gysling *et al.* [5] showed that the Schulz–Flory plots for CO hydrogenation on $LaRhO_3$ are essentially equivalent to those found for Rh–SiO_2 suggesting the same catalytically active centre (Rh^0) for both catalysts. Watson and Somorjai [1] and Somorjai and Davis [2] found that selectivity to formation of hydrocarbons and oxygenates from CO + H_2 on $LaRhO_3$ is highly dependent on the temperature. This change in selectivity is assumed to be due to competition between processes of hydrogenation and carbonylation and to variable concentrations of molecularly and dissociatively adsorbed CO and H_2 on the surface of the perovskite. However, these authors concluded that the active catalyst contains most of the rhodium in the 1+ oxidation state with some metal present. Monnier and Apai [3] found, also, evidence suggesting that different oxidation states of copper (Cu^0 and Cu^+) are required in Cu–Cr oxide catalysts for methanol formation from syngas.

Broussard and Wade [4] examined a wide spectrum of perovskite oxides as catalysts for syngas conversion to oxygenated organic compounds. Among these, they studied $LnMO_3$ (Ln = lanthanum, neodynium; M = manganese, iron, cobalt, nickel) oxides and multicomponent perovskites containing two alkaline-earth or rare-earth metals in position A and two transition metals in position B. The perovskite $LaFeO_3$ presents the advantage of being more stable in a reducing atmosphere than the corresponding perovskites of cobalt and nickel [7–9]. For example, $LaFeO_3$ does not undergo reduction in hydrogen at 600 K. Reduction of $1e^-$ (to Fe^{2+}) and $3e^-$ (to Fe^0) per molecule occurs at much higher temperatures (1000 and 1200 K, respectively). In agreement with this Broussard and Wade [4] showed that the iron in $LaFeO_3$ after being used in syngas conversion exhibited oxidation states of 3+ in the bulk and higher than zero in the surface. They concluded that Fe^{n+} cations are the catalytic sites for this reaction.

In this work we have studied the interactions of CO, CO_2 and H_2 with $LaFeO_3$ as a function of the reduction temperature of the oxide in order to obtain information on the reactivity of this perovskite. These results should be useful to assess the role of the cation in position B and its oxidation state in the CO + H_2 reaction. The identification of the adsorbed and desorbed species has been effected by means of temperature programmed desorption (TPD) and infrared (IR) spectroscopies.

2. Experimental details

The $LaFeO_3$ sample was prepared by amorphous precursor decomposition. The precursor (metal citrates) underwent a final heat treatment at 923 K for 4 h in air. The presence of a single perovskite phase was verified by X-ray diffraction. The BET specific surface area of the sample as determined by nitrogen adsorption at 77 K was $10.0\,m^2\,g^{-1}$. Details of analysis of H_2, CO and CO_2 have been given previously [10]. Before use, these gases were further purified by standard

0022-2461/89 $03.00 + .12

methods. The carrier (He, 99.998%) for TPD was purged of its main impurity (O_2) down to less than 1 p.p.m.

The flow system used for TPD experiments has been described previously [11]. The 0.5 g sample was placed in a quartz microreactor which could be heated at programmed temperature up to 1 K sec^{-1}. The analysis of the effluent gases was made by means of a mass spectrometer UTI model 100C. The signal intensity for a series of preselected masses and the temperature of the sample were recorded with a data acquisition system. Experiments were performed after gas adsorption on oxidized and reduced samples. For oxidation a mixture of 21% O_2–79% He was passed through the sample at 823 K for 1 h. The reduced samples were prepared from oxidized $LaFeO_3$ by passing a hydrogen flow at the desired temperature (523 to 823 K) for 1 h. The samples will be referred to as $LaFeO_3$ (ox 823) and $LaFeO_3$ (red RT) where RT denotes the reduction temperature in Kelvin. After the appropriate oxidation or reduction treatment, the sample was outgassed by passing a helium flow through the microreactor at 823 K for 1 h. The adsorption of individual gases was effected by passing a flow of CO or CO_2 at 298 K for 0.5 h and then a helium flow at 298 K for 15 min for removal of the physisorbed part. CO–H_2 successive adsorption was carried out by passing flows of CO (298 K, 0.5 h), He (298 K, 15 min), H_2 (198 K, 0.5 h) and He (298 K, 15 min). H_2–CO adsorption was effected as for CO–H_2 adsorbing H_2 first and then CO. The reactor was then repressurized with helium and heating of the catalyst was started at 0.5 K sec^{-1}. Between two successive TPD runs, the sample underwent treatments of oxidation, reduction and outgassing as above. To avoid changes in specific surface area the final heating temperature of the sample was kept 100 K below the maximum temperature used for sample preparation. The flow rates used in reduction, outgassing, adsorption and TPD runs were 50 cm^3 min^{-1}.

IR spectra were recorded using a spectrophotometer Perkin–Elmer 682 with a wedge attenuator in the reference beam. Self-supporting discs were made by pressing 120 mg of powder to a pressure of 1×10^8 N m^{-2} in a 25 mm die and placed in an IR cell connected to a high vacuum system in which a pressure of 10^{-6} Torr (1 Torr = 133.3 N m^{-2}) could be maintained. As for TPD experiments, oxidized and reduced samples were studied. Oxidation was effected by heating in 700 Torr air at 773 K for 1 h. For reduction, the oxidized sample was outgassed at 773 K for 1 h and then heated in 300 Torr hydrogen at the desired temperature for 1 h (sample notation as for TPD). Prior to an experiment the sample was outgassed in high vacuum at 773 K for 1 h and then contacted with 100 Torr CO or CO_2 at 298 K for 0.5 h. Spectra were recorded in the presence of the gas, after evacuation at 298 K for 5 min and after evacuation at the specified outgassing temperature for 0.5 h.

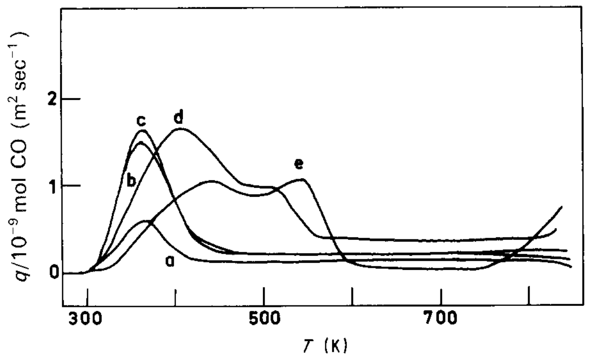

Figure 1 TPD spectra of CO after CO adsorption at 298 K on (a) oxidized $LaFeO_3$ and on $LaFeO_3$ reduced in hydrogen at (b) 523, (c) 623, (d) 723 and (e) 823 K.

3. Results and discussion

3.1. TPD results

3.1.1. CO adsorption

TPD spectra of CO after CO adsorption on $LaFeO_3$ are given in Fig. 1. CO desorption from $LaFeO_3$ (ox 823) (Fig. 1a) gives a peak at 365 K which shifts to higher desorption temperatures (to 405 K, Fig. 1d and 440 K, Fig. 1e) as the reduction temperature increases. For samples reduced at 723 and 823 K a second desorption peak appears at 495 (Fig. 1d) and 540 K (Fig. 1e), respectively. These peaks must be associated with adsorption of CO on reduced centres of iron since their intensity increases with increasing reduction temperature of the oxide. Reduction in hydrogen of bulk $LaFeO_3$ starts at temperatures above 600 K [7]. However, the surface must reduce at lower temperatures than those found for the bulk. Since no intermediate reduction state between Fe^{3+} and Fe^0 has been detected by temperature programmed reduction [7] the TPD peaks recorded were assigned to CO linearly adsorbed on metallic Fe (peak at 365 to 440 K) and to CO adsorbed in a bridged form on two metallic centres (peak at 495 to 540 K). The decrease in peak intensity observed after CO adsorption on $LaFeO_3$ (red 823) may be due to some sintering of metallic iron during the reduction process.

CO adsorption at 473 K on $LaFeO_3$ (ox 823) yielded IR bands at 2060 and 2025 cm^{-1} of linearly bound CO and at 1985 and 1930 cm^{-1} of bridged CO [12–14]. However, it was not possible to follow their evolution with the reduction temperature of the oxide because of the low transmittance of the sample. TPD and IR spectroscopic data also indicated the formation of linear and bridged species of CO after CO adsorption on similar systems, namely, $LaMnO_3$ and $LaCoO_3$ [12–14]. However, as $LaMnO_3$ is less reducible than $LaFeO_3$ [15], more oxidized centres of manganese, Mn^{n+} ($n < 3$) were assumed to participate in the adsorption process.

TPD spectra of CO_2 after CO adsorption are given in Fig. 2. They contain two broad desorption peaks centred at 570 and 715 K whose intensities decrease with the reduction temperature of the oxide. No CO_2 desorption was recorded after CO adsorption on $LaFeO_3$ (red 723) and $LaFeO_3$ (red 823). The desorbed CO_2 should arise from CO oxidation via formation and decomposition of carbonates of different thermal stability, namely, monodentate (peak at 570 K) and bidentate (peak at 715 K) carbonates. IR bands assigned to these species were found previously after

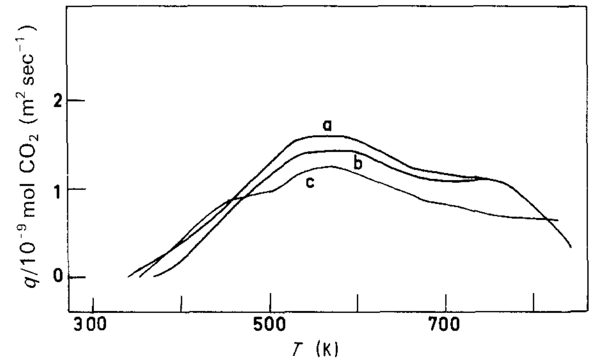

Figure 2 TPD spectra of CO_2 after CO adsorption at 298 K on (a) oxidized $LaFeO_3$ and on $LaFeO_3$ reduced in hydrogen at (b) 523 and (c) 623 K.

CO adsorption on $LaFeO_3$ (ox 823) [12–14]. The concentration of both types of carbonates decreases as the availability of surface oxygen decreases, i.e., with increasing reduction degree of the oxide. The dissimilarity of the TPD spectra of CO_2 obtained after CO (Fig. 2) and CO_2 (Fig. 3) adsorption rules out any mechanism involving direct oxidation of CO to CO_2 by oxygen of the perovskite surface previously to the formation of carbonates from the so-formed CO_2.

Coverages of CO measured from TPD peaks of CO and CO_2 (Figs 1 and 2) are given in Table I. These were calculated taking as cross-sectional area of the CO molecule the mean value (0.151 nm^2) obtained from CO adsorption on several adsorbents between 77 and 195 K [16]. From the oxidized sample only a small fraction of CO (less than 15%) is desorbed as CO and, therefore, formation of carbonates is predominant. However, with increasing reduction of the perovskite the CO adsorption in a linear or bridged form is favoured and the carbonate species decrease in concentration and eventually disappear for reduction temperatures of 723 K and above.

3.1.2. CO_2 adsorption

TPD spectra of CO_2 obtained after CO_2 adsorption are shown in Fig. 3. The peak at 425 K for $LaFeO_3$ (ox 823) (Fig. 3a) decreases in intensity and shifts to lower desorption temperatures for increasing reduction temperature of the oxide (to 375 K for $LaFeO_3$ (red 823), Fig. 3e). Note that although peaks a and b have different heights they have comparable areas. A wide tail centred at 575 to 675 K for $LaFeO_3$ (ox 823) and for samples reduced at 523 to 723 K (Figs 3a to d) becomes a well defined peak at 570 K for $LaFeO_3$ (red 823) (Fig. 3e, solid line).

TABLE I CO coverage, θ*, measured from CO and CO_2 desorption peaks after CO adsorption on $LaFeO_3$

Sample	θ	
	CO desorption	CO_2 desorption
$LaFeO_3$ (ox 823)	0.07	0.44
$LaFeO_3$ (red 523)	0.14	0.40
$LaFeO_3$ (red 623)	0.14	0.38
$LaFeO_3$ (red 723)	0.30	0
$LaFeO_3$ (red 823)	0.22	0

*Cross-sectional area of the CO molecule, 0.151 nm^2

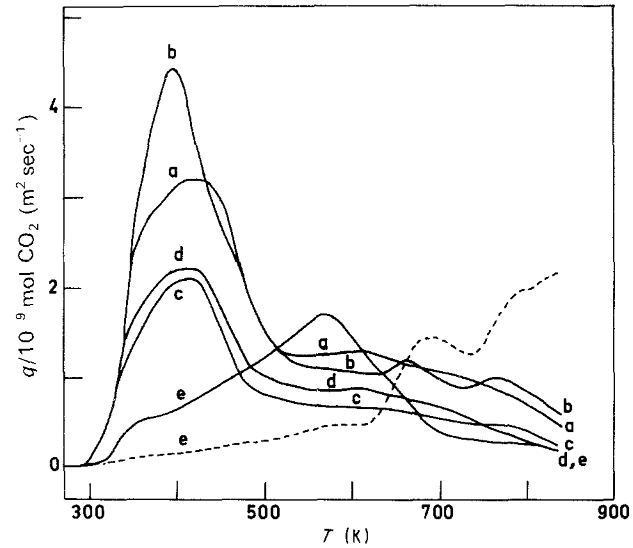

Figure 3 TPD spectra of CO_2 (full curves) or CO (broken curve) after CO_2 adsorption at 298 K on (a) oxidized $LaFeO_3$ and on $LaFeO_3$ reduced in hydrogen at (b) 523, (c) 623, (d) 723 and (e) 823 K.

CO_2 adsorption on $LaFeO_3$ (red 823) yielded also a TPD peak of CO at 690 K and an additional CO desorption above 735 K (Fig. 3e, broken line). These desorptions occur at different temperatures from those of CO_2 desorption and therefore should be due to reduction of CO_2 by reduced $LaFeO_3$. This CO desorption was not observed on less reduced samples. The oxidized as well as the reduced samples of $LaFeO_3$ adsorbed larger amounts of CO_2 than of CO. This should be related to the more acidic character of CO_2 and suggests that carbonates formed from CO_2 adsorption interact preferentially with La^{3+} cations of strong basic character.

3.1.3. Coadsorption of CO and H_2

TPD spectra of CO after CO–H_2 or H_2–CO successive adsorption on $LaFeO_3$ (red 823) were similar to those obtained after CO adsorption (Fig. 1). Therefore, hydrogen adsorption has no influence on the adsorption of CO on this reduced oxide unlike the effects observed in the successive adsorption CO–H_2 on $LaMnO_3$ (red 873) and $LaCoO_3$ (red 773) [12–14]. It should be noted, however, that hydrogen adsorption on reduced $LaFeO_3$ has been found to be a minimum within the series of $LaMO_3$ (M = chromium, manganese, iron, cobalt, nickel) oxides [17]. This would make any eventual interaction between adsorbed CO and H_2 more difficult to observe on $LaFeO_3$ than on $LaMnO_3$ or $LaCoO_3$.

TPD spectra of hydrogen recorded after CO–H_2 and H_2–CO successive adsorption on $LaFeO_3$ (red 823) are shown in Figs 4a and b. In both sequences, a similar pattern of spectra was found, i.e., a small peak at 345 to 360 K and a larger peak at higher temperatures (585 to 590 K). If we compare these spectra with that of hydrogen desorption after hydrogen adsorption alone on the same sample (Fig. 4, dashed line) [17] we can see that the lower temperature peak corresponds to that observed for hydrogen desorption in the absence of CO but its intensity has decreased considerably. The spectra shown in Figs 1 and 2 suggest

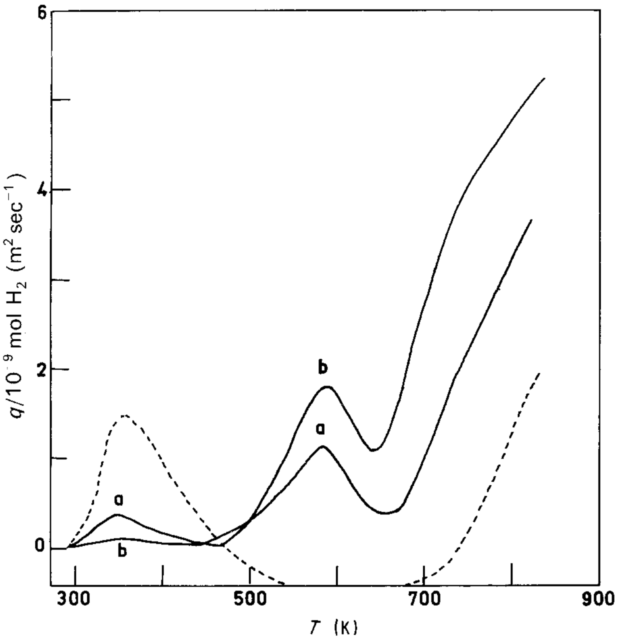

Figure 4 TPD spectra of hydrogen after (a) CO–H_2 and (b) H_2–CO successive adsorption at 298 K on $LaFeO_3$ reduced in hydrogen at 823 K. Broken curve, TPD spectrum of hydrogen after hydrogen adsorption at 298 K on the same absorbent.

that CO adsorbs on metallic iron in the system CO–$LaFeO_3$ (red 823). On the other hand, the TPD peak of hydrogen at 345 to 360 K recorded after hydrogen adsorption on $LaFeO_3$ reduced in the temperature interval 523 to 823 K increased in intensity with increasing reduction temperature indicating that hydrogen adsorption takes place on reduced iron centres, presumably metallic iron [17]. The coadsorption results seem to indicate that CO and hydrogen compete for the same type of centre. In line with this reasoning it can be inferred that CO occupies Fe^0 centres and therefore inhibits hydrogen adsorption (CO–H_2 sequence, Fig. 4a) or displaces adsorbed hydrogen from Fe^0 to a new adsorption site (H_2–CO adsorption, Fig. 4b). Therefore CO interacts more strongly than hydrogen with the adsorbent surface.

The question arises about which type of centres adsorb the hydrogen producing the higher temperature peak of the TPD spectra after both successive adsorption sequences (Fig. 4). On the one hand, a higher desorption temperature means a stronger interaction between hydrogen and the adsorption centres. This would imply that if such centres were present in the perovskite in the absence of CO, they would be filled with hydrogen faster than those with a weaker interaction, thus producing either two peaks or only the peak corresponding to the higher energy of interaction (higher desorption temperature). No such peak appears in the spectrum obtained after hydrogen adsorption (Fig. 4, broken line). Therefore, the formation of the new adsorption centres for hydrogen, causing the higher temperature TPD peak seems to be favoured by the presence of CO. On the other hand, the sum of the integrated surfaces of both peaks in the TPD spectra of both successive adsorptions is roughly equal to that of the unique peak in the spectrum of hydrogen adsorption which could indicate that the total number of adsorption centres for hydrogen has not changed. Then, one can speculate that, as CO occupies Fe^0 centres or displaces hydrogen from these centres, hydrogen would then adsorb on the moiety "Fe^0–CO" probably through a C–H or an O–H bond. This entity "Fe^0–CO–H" could be an intermediate in the formation of oxygenates. Unfortunately, the transmission of $LaFeO_3$ (red 823) to IR radiation is too low for wavenumbers above 2300 cm^{-1} and therefore no reliable information in the spectral region corresponding to the bands associated to C–H or O–H bonds can be obtained. Thus the structure of the proposed "Fe^0–CO–H" entity can not be described in more detail.

As stated above, hydrogen adsorption (in absence of CO) on $LaFeO_3$ is a minimum within the $LaMO_3$ series of oxides. However, the CO conversion in CO + H_2 reaction on $LaFeO_3$ at 593 K lies between the values measured on $LaMnO_3$ and $LaCoO_3$ at the same temperature [4]. This absence of parallelism between adsorption and conversion can be accounted for on the basis of the above results, since the nature of the bond of the adsorbed hydrogen with the oxide surface is strongly dependent on the presence or absence of CO.

3.2. Infrared spectroscopic results

Infrared spectra obtained after CO_2 adsorption at 298 K on oxidized $LaFeO_3$ and $LaFeO_3$ reduced in hydrogen at 523 to 773 K are given in Fig. 5. On the oxidized sample, bands at 1600, 1325, 1218, 1050 and 840 cm^{-1} corresponding to carbonate species were observed (Fig. 5a). The wide bands at 1600 and 1325 cm^{-1} decrease in intensity while the band at 1050 cm^{-1} increase in intensity with increasing reduction temperature of the oxide (Figs 5a to d). Therefore, these bands should be associated to two different carbonate species. The intensities of the

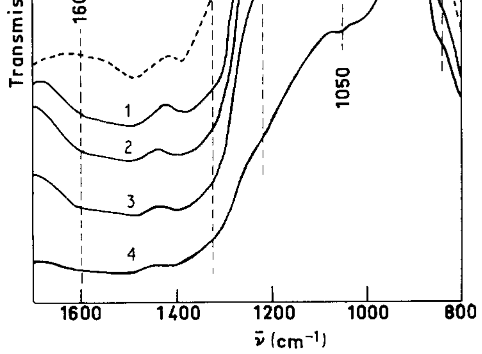

Figure 5 Infrared spectra, in the presence of the gaseous phase, after admission of 100 Torr CO_2 for 0.5 h at 298 K on (1) oxidized $LaFeO_3$ and on $LaFeO_3$ reduced in hydrogen (2) 523, (3) 723 and (4) 773 K. Broken curve, background spectrum.

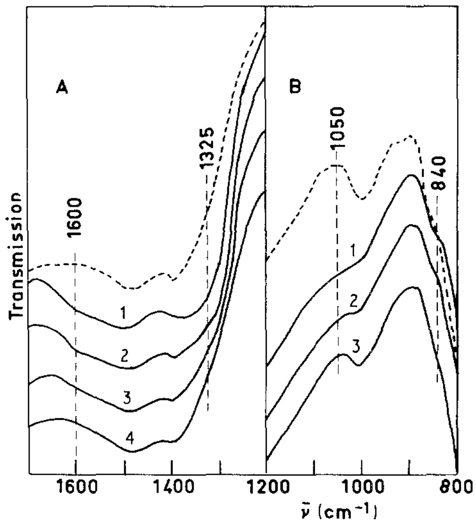

Figure 6 (a) Infrared spectra after admission of 100 Torr CO_2 for 0.5 h at 298 K on $LaFeO_3$ reduced in hydrogen at 523 K and outgassing for 5 min at (1) 298, 0.5 h at (2) 373, (3) 473 and (4) 573 K. (b) Infrared spectra after admission of 100 Torr CO_2 for 0.5 h at 298 K on $LaFeO_3$ reduced in H_2 at 773 K and outgassing for 0.5 h at (1) 373, (2) 473 and (3) 673 K. Broken curves, background spectrum.

bands at 1218 and 840 cm^{-1} remain constant for all the samples.

Infrared spectra obtained after CO_2 adsorption at 298 K and outgassing at increasing temperatures are given in Fig. 6. $LaFeO_3$ (red 523) and $LaFeO_3$ (red 773) were chosen as adsorbents since after dosing with CO_2 they yielded carbonate bands of high intensity in the high and low region of the spectrum, respectively. The band at 1218 cm^{-1} is unrelated to the others since it disappears from the spectrum while those at 1600, 1325, 1050 and 840 cm^{-1} remain after pumping for 5 min at 298 K (Fig. 6a, 1). The bands at 1600 and 1325 cm^{-2} (CO_2-$LaFeO_3$ (red 523)) decrease significantly in intensity after outgassing at 473 K (Fig. 6a, 3) and are completely removed from the spectrum after outgassing at 573 K (Fig. 6a, 4). The bands at 1050 and 840 cm^{-1} (CO_2-$LaFeO_3$ (red 773)) remain practically unmodified after outgassing at 373 and 473 K (Fig. 6b, 1, 2) and are eliminated after outgassing at 673 K (Fig. 6b, 3). Therefore the carbonate species associated with the band at 1050 cm^{-1} exhibits a higher thermal stability than the species associated with bands at 1600 and 1325 cm^{-1}.

3.3. Surface species and reactivity

Although CO_2 is highly stable its reactivity with oxides to yield carbonates is higher than that of CO since formation of such species from the former molecule needs only one additional metal-oxygen (M–O) bond while two additional M–O bonds should be formed from CO. Thus, the amount of adsorbed CO_2 measured on $LaFeO_3$ was higher than that for CO. On the other hand, no carbonates were formed (absence of TPD peaks of CO_2) after CO adsorption at 298 K on $LaFeO_3$ reduced at 723 and 823 K (Fig. 2, Table I) while carbonates formation was observed by TPD (Fig. 3) and IR (Fig. 5) spectroscopies after CO_2 adsorption on $LaFeO_3$ (red 823) and $LaFeO_3$ (red 773), respectively. Carbonates formation from CO is highly enhanced by adsorption at 473 K and above [12–14].

The decrease in intensity of the infrared bands at 1600 and 1325 cm^{-1} recorded after CO_2 adsorption at 298 K (Fig. 5) as the reduction temperature of the perovskite increases suggests formation of a monodentate carbonate. These bands are due to the splitting of the doubly degenerate ν_3 (antisymmetric CO stretching) vibration of the free carbonate ion upon coordination [18]. For the system under study $\Delta\nu_3 = 275\ cm^{-1}$ although the breadth of the bands does not allow its accurate determination. $\Delta\nu_3$ for monodentate carbonates is usually not higher than 200 cm^{-1}. However, higher values have been reported for CO_2 adsorption on CaO [19], Al_2O_3 [20], TiO_2 [21] and NiO [22]. This carbonate species should be associated to the TPD CO_2 peak at 375 to 425 K obtained after CO_2 adsorption because both TPD (Fig. 3) and IR (Fig. 5) signals disappear from the spectrum at about the same reduction temperature increases. Moreover, these signal disappear from the spectrum at about the same temperature (Figs 3 and 6).

The band at 1050 cm^{-1} is assigned to the ν_1 vibration (symmetric CO stretching) of a carbonate species of a higher thermal stability than that of the above described species, such as a bidentate carbonate. Formation of this type of carbonate from CO_2 takes place on pairs of surface sites composed of a lattice oxygen and an anionic vacancy [23]. The increase in intensity of this band with increasing reduction temperature of $LaFeO_3$ (Fig. 5) is consistent with this interpretation. This carbonate species should be associated to the TPD tail or peak at 570 to 675 K of CO_2 obtained after CO_2 adsorption since both TPD (Fig. 3) and IR (Fig. 5) signals increase with increasing reduction temperature and they are eliminated from the spectra at higher temperatures than the signals attributed to monodentate carbonates (Figs 3 and 6). The band at 1218 cm^{-1} is indicative of the presence of a very labile carbonate since it is removed from the perovskite surface by pumping at 298 K. Formation of monodentate and bidentate carbonates were reported by Udovic and Dumesic in the system CO_2-Fe_3O_4 [24].

4. Conclusions

TPD spectra of CO after CO adsorption on $LaFeO_3$ at 298 K presented peaks which are assigned to CO absorbed in a linear and a bridged form on metallic iron. Adsorption of CO and CO_2 yielded CO_2 desorption peaks attributed to monodentate and bidentate carbonates.

TPD spectra obtained after CO and H_2 successive adsorption on reduced $LaFeO_3$ indicate that CO and hydrogen compete for the same type of centre. CO occupies Fe^0 centres and therefore inhibits hydrogen adsorption (CO–H_2 sequence) or displaces hydrogen from these centres (H_2–CO sequence). Hydrogen, then, adsorbs on the moiety "Fe^0–CO" yielding a "Fe^0–CO–H" species. This entity may be an intermediate in the formation of oxygenates from CO and H_2. The interaction of CO with the adsorbent surface is therefore stronger than that of hydrogen.

Although CO showed reactive adsorption on $LaFeO_3$

at 298 K yielding CO and carbonate species it was not large enough to observe the evolution of these species with the reduction temperature of the perovskite by means of infrared spectroscopy. The reactivity of CO is highly enhanced at adsorption temperatures of 473 K and above. The results obtained seem to indicate that anion vacancies in the oxide lattice play an important role in the formation of carbonates from CO_2.

Acknowledgement

This work was carried out under the sponsorship of the Spanish–North American Joint Committee for Scientific and Technological Cooperation (Project No. CCB8409-003) to whom the authors gratefully acknowledge the financial assistance received.

References

1. P. R. WATSON and G. A. SOMORJAI, *J. Catal.* **74** (1982) 282.
2. G. A. SOMORJAI and S. M. DAVIS, *CHEMTECH* **13** (1983) 502.
3. J. R. MONNIER and G. APAI, *Preprints, Am. Chem. Soc., Div. Fuel Chem., New York* **31** (1986) 239.
4. J. A. BROUSSARD and L. E. WADE, *ibid.* **31** (1986) 75.
5. H. J. GYSLING, J. R. MONNIER and G. APAI, *J. Catal.* **103** (1987) 407.
6. M. A. ULLA, R. A. MIGONE, J. O. PETUNCHI and E. A. LOMBARDO, *ibid.* **105** (1987) 107.
7. J. M. D. TASCÓN, J. L. G. FIERRO and L. G. TEJUCA, *J. Chem. Soc., Faraday Trans. 1* **81** (1985) 2399.
8. M. CRESPIN and W. K. HALL, *J. Catal.* **69** (1981) 359.
9. J. L. G. FIERRO, J. M. D. TASCÓN and L. G. TEJUCA, *ibid.* **93** (1985) 83.
10. J. S. RIECK and A. T. BELL, *ibid.* **96** (1985) 88.
11. G. C. LOW and A. T. BELL, *ibid.* **57** (1979) 397.
12. L. G. TEJUCA, C. H. ROCHESTER, J. L. G. FIERRO and J. M. D. TASCÓN, *J. Chem. Soc., Faraday Trans. 1* **80** (1984) 1089.
13. L. G. TEJUCA, A. T. BELL, J. L. G. FIERRO and J. M. D. TASCÓN, *ibid.* **83** (1987) 3149.
14. L. G. TEJUCA, A. T. BELL, J. L. G. FIERRO and M. A. PEÑA, *Appl. Surf. Sci.* **31** (1988) 301.
15. J. L. G. FIERRO, J. M. D. TASCÓN and L. G. TEJUCA, *J. Catal.* **89** (1984) 209.
16. A. L. McCLELLAN and H. F. HARNSBERGER, *J. Colloid Interface Sci.* **23** (1967) 577.
17. L. G. TEJUCA, *Thermochim. Acta* **126** (1988) 205.
18. G. BUSCA and V. LORENZELLI, *Mater. Chem.* **7** (1982) 89.
19. Y. FUKUDA and K. TANABE, *Bull. Chem. Soc. Jpn* **46** (1973) 1616.
20. C. MORTERRA, S. COLUCCIA, G. GHIOTTI and A. ZECCHINA, *Z. Phys. Chem.* **104** (1977) 275.
21. C. MORTERRA, A. CHIORINO, F. BOCCUZZI and E. FISICARO, *ibid.* **124** (1981) 211.
22. R. P. EISCHENS and W. A. PLISKIN, *Adv. Catal.* **9** (1957) 662.
23. M. P. ROSYNEK and D. T. MAGNUSON, *J. Catal.* **48** (1977) 417.
24. T. J. UDOVIC and J. A. DUMESIC, *ibid.* **89** (1984) 314.

Received 21 September 1988
and accepted 24 February 1989